Density functional theory study of the partial oxidation of methanol on copper surfaces

Sung Sakong and Axel Groß
Physik Department T30g, Technische Universität München, James-Franck-Straße, 85747 Garching/Germany

The partial oxidation of methanol to formaldehyde on clean and oxygen-precovered Cu(100) and Cu(110) has been studied by density functional theory calculations within the generalized gradient approximation. We have determined the geometric and electronic structure of the reaction intermediates. Methanol and formaldehyde are only relatively weakly bound to copper while methoxy is strongly chemisorbed. Still, we have identified a highly deformed formaldehyde species strongly interacting with Cu(100) and Cu(110). The reaction paths have been determined using the nudged elastic band method. It turns out that the rate-limiting step is the dehydrogenation of methoxy to formaldehyde which is hindered by a significant activation barrier. While dosing with oxygen does not reduce this barrier, it still facilitates this reaction by stabilizing the methoxy intermediate on the Cu surface and causing the removal of surface hydrogen via water desorption. Tensile strain of the copper substrate leads to enhanced total binding energies of all reaction intermediates, but there is no clear trend, as far the height of reaction barriers as a function of the strain in concerned.

I. INTRODUCTION

Both the methanol decomposition and synthesis are industrially important processes. The methanol steam reforming process has been suggested as an efficient source to generate hydrogen in the context of fuel cell technology [1, 2]. On the other hand, methanol is one of the most important synthetic chemicals. Industrially, methanol synthesis and decomposition are catalysed by Al_2O_3-supported Cu/ZnO [3]. Despite extensive studies, the precise state of the copper and the role of the ZnO in the Cu/ZnO-catalysts is still unclear. The active phase has been suggested to be either copper dissolved in the bulk [4] or metallic copper dispersed on the ZnO surface [5, 6].

Recently, it was shown that the activity of methanol synthesis can be directly correlated with the microstrain of the copper metal particles [7]. It was furthermore suggested that the strain might be induced by a metastable suboxide species penetrating the copper matrix [8]. The strong influence of strain on the adsorption properties of metal surfaces has already been shown in a number of experimental and theoretical studies [9–17]. In general, metal surfaces under tensile strain respond by an upshift of the local d-band which leads to a stronger interaction with adsorbates according to the so-called d-band model [18].

Due to the important role of copper in the synthesis and steam reforming of methanol, the interaction of methanol with low-index copper surfaces has been the subject of many studies following the classical temperature-programmed desorption (TPD) experiments by Madix and co-workers on Cu(110) [19, 20] more than 20 years ago. The reaction pathways proposed in these studies have basically remained valid in spite of numerous successive experiments [21–31].

Clean copper surfaces exhibit a relatively low activity for methanol oxidation. At low surface temperatures of about 100 K only adsorbed methanol is present at Cu surfaces [21, 31]. For higher temperatures first methoxy and then formaldehyde is formed although there is some controversy about the exact temperatures at which this happens [21, 31]. Further heating above 300 K leads to the desorption of formaldehyde and the associative desorption of hydrogen and methoxy as methanol.

The presence of oxygen on copper strongly promotes the decomposition of methanol [19, 21]. Methanol is converted to methoxy on copper predosed with oxygen via the formation of surface hydroxyl. Secondary ion mass spectrometry (SIMS) experiments show explicitly the combined increase of the methoxy and hydroxyl signal as a function of methanol exposure [30] at 130 K. Further methanol interacts with the adsorbed hydroxyl species to produce water which then desorbs, as can be deduced from high resolution X-ray photoelectron spectra (HRXPS) recorded at 220 K [31]. Under low remaining oxygen coverage, the methoxy adsorbates are decomposed to form formaldehyde and atomic hydrogen at 330-400 K [19, 24]. For higher oxygen coverages, also the formation of formate is observed [26, 27, 32] which is followed by CO_2 production.

A more detailed picture of the methanol decomposition process on oxygen-covered copper surfaces has been provided by STM studies. Methoxy forms stable (5×2) and $c(2 \times 2)$ superstructures on oxygen-covered Cu(110) [22, 29]. The methoxy-covered regions are well-seperated from oxygen-covered 2×1 islands. The development of the ordered methoxy structures is accompanied by the removal of oxygen from the (2×1)O islands [29]. The subsequent disappearance of the methoxy islands driven by further oxygen exposure has been associated with the first step in the decomposition of methoxy to formaldehyde.

The methanol dehydrogenation on copper has also been studied theoretically by electronic structure calculations, mainly on clean Cu(111) where the methanol decomposition is hindered by large reaction barriers. Using a cluster approach, the methoxy intermediate on Cu(111) has been addressed on the Hartree-Fock and configuration interaction level [33]. Hartree-Fock based methods were also used in a cluster study of the methanol synthesis on Cu(100) [34]. Gomes *et al.* have studied the methoxy radical reaction to formaldehyde and the adsorption properties of the intermediates of the methanol oxidation on Cu(111) using density functional theory (DFT) [35, 36], but again using a cluster to model the Cu substrate. The thermochemistry of the stable intermediates on Cu(111) plus the abstraction of hydrogen from methoxy was the subject of a recent periodic DFT study [37].

In order to obtain a microscopic picture of the methanol oxidation process on Cu(100) and Cu(110), we have performed periodic DFT calculations within the generalized gradient approximation [38]. The geometric and electronic structure of the reaction intermediates has been carefully analysed. We have identified a chemisorbed formaldehyde species that has not been found before on Cu surfaces to the best of our knowledge. We have determined the reaction paths for the partial oxidation of methanol to formaldehyde both on clean as well as on oxygen-precovered Cu surfaces. In addition, we discuss strain effects of the copper substrate in the methanol decomposition process.

II. METHODS

The DFT calculations have been performed using the Vienna *ab initio* simulation package (VASP) [39]. The exchange-correlation effects have been described within the generalized gradient approximation (GGA) using the Perdew-Wang (PW91) functional [38]. The ionic cores are represented by ultrasoft pseudopotentials [40] as constructed by Kresse and Hafner [41]. While for copper a cutoff energy for the plane wave expansion of 350 eV is sufficient, methanol requires an cutoff energy of 600 eV to obtain fully converged results. However, already at 320 eV the error for the free methanol molecule is below 10 meV. Hence we have chosen a cutoff energy of 350 eV for all results reported in this study which yields sufficient accuracy.

The electronic structure of the studied molecules has been analysed by determiming the orbital projected density of states. In the assignment of the molecular orbitals we have followed the general quantum chemistry naming rules. a and b correspond to non-degenerate and e to doubly degenerate molecular orbitals, respectively, while the subscripts 1 and 2 denote the symmetry properties of the orbitals with respect to the corresponding bond. The density of states of the free molecules and the adsorbed molecules are compared by aligning the vacuum energy of the electrons.

The Cu substrates are modeled by a slab of 5 layers which are separated by 12 Å vacuum. In all calculations, the uppermost two Cu layers are fully relaxed. Most results reported here have been obtained for 2×2 surface unit cells. We have used a relatively fine Monkhorst-Pack **k**-point mesh of 16×16×1 which is necessary in order to obtain converged energies since the Fermi energy lies in a region of a low Cu density of states [13].

The adsorption energy of each species is defined as

$$E_{\text{ads}}^{\text{mol}} = E_{\text{total}}^{\text{slab+adsorbates}} - (E_{\text{slab}} + E_{\text{gas}}^{\text{mol}}) \ , \qquad (1)$$

where $E_{\text{total}}^{\text{slab+adsorbates}}$ is the total energy of the interacting system of slab and adsorbates. $E_{\text{gas}}^{\text{mol}}$ is the gas-phase energy of each molecular species and E_{slab} the energy of the isolated slab. According to this definition, exothermic adsorption corresponds to negative adsorption energies. In the following, we will refer to the absolute value of the adsorption energy as the binding energy. If more than one methanol molecule is involved in a particular reaction scheme, we define the reference energy E_{ref} as

$$E_{\text{ref}} = E_{\text{slab}} + n\, E_{\text{gas}}^{\text{CH}_3\text{OH}} \ , \qquad (2)$$

where n is the number of involved methanol molecules and $E_{\text{gas}}^{\text{CH}_3\text{OH}}$ is the gas-phase methanol energy.

The minimum energy paths are determined using the nudged elastic band (NEB) method developed by Jónsson *et al.* [42–45]. In particular, we have used the climbing image NEB method[45] and also the dimer method [46] in order to determine the geometries of the transition states.

III. RESULTS

A. Geometric and electronic structure of reaction intermediates

Detailed DFT calculations have been performed in order to determine the minimum energy structures of the reaction intermediates in the partial oxidation of methanol on Cu(100) and Cu(110). The adsorption geometries of methanol, methoxy and formaldehyde in various configurations and their adsorption energies are listed in Table I. First of all it is obvious that the closed-shell species methanol (CH_3OH) and formaldehyde (CH_2O) are only relatively weakly bound to the copper surface while the open-shell methoxy radical (CH_3O) is strongly interacting with Cu.

Experimentally, the adsorption energies of methanol and formaldehyde have been derived from temperature programmed desorption (TPD) data assuming first-order desorption and a prefactor of $\nu = 10^{13}$ s^{-1}. For methanol this yields adsorption energies of −0.56 eV on Cu(111) [47], −0.43 eV on Cu(100) [48] and −0.70 eV on Cu(110) [19], while for formaldehyde one obtains −0.33 eV on Cu(111) [49] and −0.56 eV on Cu(110) [19]. Typically, the measured binding energies for the weakly bound species are somewhat larger than the DFT results determined by us and others [35–37] with the exception of formaldehyde on Cu(110).

In detail, we find that methanol is only weakly bound to Cu(100) and Cu(110). The analysis of the electronic structure of adsorbed methanol yields that the molecular orbitals remain narrow and that they are only slightly shifted with respect to their position in gas phase. Hence methanol can be regarded as being only physisorbed at clean copper surfaces. Consequently, methanol is adsorbed rather far away from the surface, and there is only a small variation in the binding energy with the adsorption site. The hydroxyl bond (O-H) of methanol is oriented parallel to the surface, the C-O bond is almost upright and the oxygen atom prefers sites with a high electron density. On Cu(110), the electron density is more strongly varying than on Cu(100) leading to a higher binding energy of methanol.

The open-shell methoxy radical (CH_3O), on the other hand, is strongly interacting with clean copper surfaces. In Fig. 1, the projected local density of states of the oxygen atom of methoxy adsorbed on Cu(100) (a) and Cu(110) (b) is shown. On Cu(100), methoxy prefers the high symmetry site, namely the four-fold hollow site [50]. On Cu(111), methoxy is also adsorbed at the high-symmetry hollow site, however, with a weaker binding by 0.3 eV [37]. In the gas-phase, the $2e$ orbital which corresponds to a nonbonding π orbital on oxygen is only partially filled [51]. As Fig. 1 shows, this $2e$ orbital is significantly broadened by the direct coupling to the Cu d-states which causes the high adsorption energy. Furthermore, the p_z ($5a_1$) orbital is shifted down by about 2 eV even below the degenerate p_x and p_y ($1e$) states. This leads to an $1e/5a_1$ orbital inversion, which has already been observed in experiment [52] and also been confirmed by semi-empirical cluster calculation [53] on Cu(111).

Adsorbate	Substrate	Site	$E_{\rm ads}$(eV)	$h_{\rm Cu-O}$(Å)	$d_{\rm Cu-O}$(Å)
CH_3OH	Cu(100)	O_t-H_b	−0.18	2.24	2.27
		O_t-H_h	−0.21	2.20	2.23
		O_b-H_h	−0.19	2.46	2.84
	Cu(110)	O_{sb}-H_h	−0.35	1.84	2.34
		O_t-H_{lb}	−0.41	2.02	2.18
CH_3O	Cu(100)	O_h	−2.96	1.12	2.18
	Cu(110)	O_{sb}	−2.98	1.44	1.95
		O_{lb}	−2.61	1.14	2.04
	Cu(111)	O_{fcc}	−2.68	1.45	2.08
					$d_{\rm C-O}$(Å)
CH_2O	Cu(100)	C_b-O_b	−0.70	1.42	1.41
		-	−0.14	3.00	1.24
	Cu(110)	C_{sb}-O_{sb}	−0.63	1.17	1.41
		O_{sb}	−0.21	1.72	1.27
		−	−0.10	2.75	1.25

TABLE I: Molecular adsorption energies $E_{\rm ads}$, adsorption height of the oxygen atom $h_{\rm Cu-O}$ with respect to the uppermost Cu plane and minimum O-Cu distance $d_{\rm Cu-O}$ for various $p(2\times2)$ adsorption configurations over pure Cu(100), Cu(110) and Cu(111). The adsorption sites are characterized with respect to the oxygen, hydroxyl hydrogen and carbon position within the surface unit cell. t, b and h denote the top, bridge and hollow sites while sb and lb stand for the short-bridge and long-bridge sites of the (110) surface, respectively.

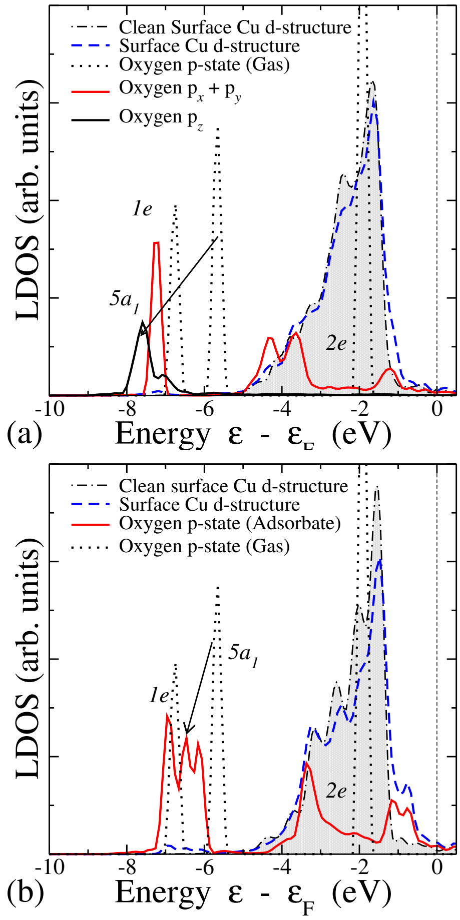

FIG. 1: Projected local density of states (LDOS) of the oxygen atom of methoxy on (a) the four-fold hollow site of Cu(100) and (b) the pseudo (111) edge of Cu(110). Remarkable features are the $5a_1/1e$ orbital inversion on Cu(100) (a) and the splitting of the $1e$ orbital on Cu(110) (b).

On Cu(110), the bonding situation of methoxy is different from the Cu(111) and Cu(100) cases. The adsorption geometry is shown in Fig. 2. Our results confirm the experimental findings [54, 55]. At its most favorable adsorption position, methoxy is located at the short bridge site with the CO bond tilted by 33° along [001] from the (110) surface normal. This can be described as a pseudo (111) surface edge position with the CO bond tilted by 2° from the pseudo Cu(111) surface normal. The adsorption height with respect to the pseudo (111) surface is smaller than on pure Cu(111) and the adsorption stronger. Similar adsorption configurations are also found on (110) surfaces for other systems such as CH_3O/Ni(110) [56] and NO/Pd(110) [57]. The adsorption site at the pseudo (111) surface edge position does not correspond to a high-symmetry situation. This is also reflected by the local density of states. The oxygen p_x and p_y ($1e$) states are no longer degenerate. The $1e$ peak is split in two with the downshifted $5a_1$ orbital

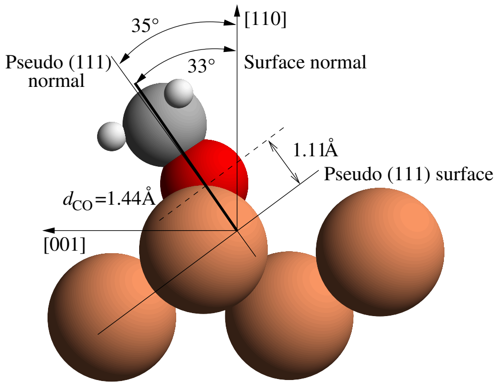

FIG. 2: Calculated adsorption geometry of methoxy on Cu(110)

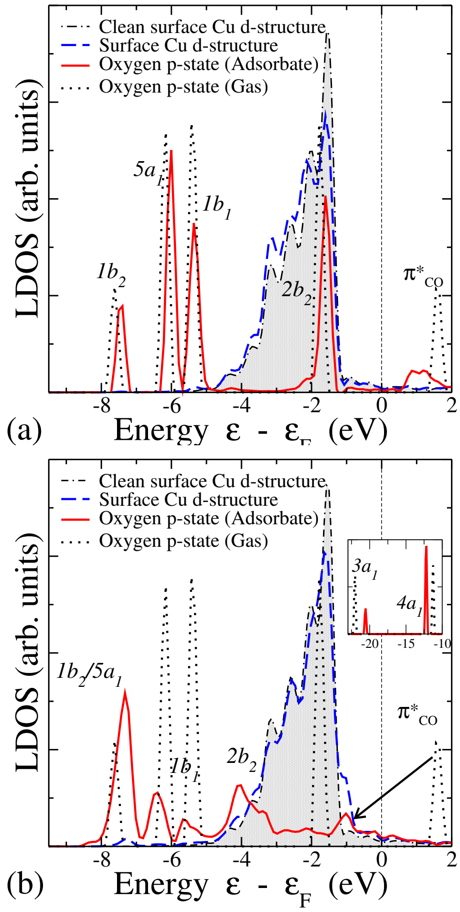

FIG. 3: Projected local density of states (LDOS) of the oxygen atom of formaldehyde adsorbed on Cu(110): a) physisorbed formaldehyde, b) chemisorbed formaldehyde.

located between the two $1e$-derived peaks.

If Cu(110) is exposed to mixtures of oxygen and methanol, oxygen-covered areas coexisting with methoxy zigzag chains and $c(2\times2)$ structures have been found by STM experiments [29]. In fact, we also find an attractive interaction between the adsorbed methoxy radicals on Cu(110): the binding energy of methoxy in the $c(2\times2)$ structure is 0.1 eV larger per molecule than in the $p(2\times2)$ structure which is listed in Table I. However, the adsorption geometry is almost the same for both coverages.

Finally, we discuss the adsorption of formaldehyde (CH_2O) on Cu(100) and Cu(110). As Table I reveals, several adsorption geometries with relatively small adsorption energies exist. However, there are significant differences in the bonding characteristics between the various adsorption positions. On both Cu(100) and Cu(110), very weakly physisorbed formaldehyde species exist about 3 Å away from the surface. This state is almost independent from the lateral position. As Fig. 3a shows, the molecular orbitals remain almost unchanged upon physisorption. Then there is the η^1 state of formaldehyde on Cu(110) above the short-bridge site which is slightly stronger bound than the physisorbed species.

Furthermore, we have identified even stronger bound η^2-formaldehyde species on both Cu(100) and Cu(110) which are in fact significantly interacting with the substrate. This strong interaction is demonstrated in Fig. 3b, where the projected LDOS at the oxygen atom of formaldehyde on Cu(100) is shown. In this adsorption geometry, the CO bond is oriented parallel to the surface and elongated from 1.22 Å in the gas phase to 1.41 Å, i.e. by 0.19 Å. This elongation of the $\pi_{\mathrm{C-O}}$ bond is reflected by the strong decrease in the intensity of the corresponding $1b_1$ peak. The $\sigma_{\mathrm{C-O}}$ ($3a_1$) and $\sigma_{\mathrm{CH_2}}$ ($4a_1$) orbitals (see the inset of Fig. 3b) are shifted to positions adequate for methoxy. In particular the $1b_2$ orbital is strongly hybridized with the Cu d-band reflecting the strong interaction between the formaldehyde and the substrate.

The geometry of the chemisorbed formaldehyde on Cu(110) is illustrated in the charge density difference plots shown in Fig. 4. Formaldehyde is adsorbed above the troughs running along the $[1\bar{1}0]$ direction with the C-O axis oriented perpendicular to the troughs. The charge distribution clearly shows the charge depletion between the C and the O atom of the adsorbed formaldehyde. This indicates the bond weakening of the C-O bond in real space.

In fact, the configuration of the chemisorbed η^2-formaldehyde can be interpreted as a formaldehyde molecule within the geometry of a free methoxy radical except for the missing methyl hydrogen atom. The C-O bond length and the CH_2 configuration are methoxy-like. We calculated that in the gas-phase it requires 1.65 eV to bring the free formaldehyde molecule into the configuration of the adsorbed molecule. Hence one can regard this strongly interacting formaldehyde molecule as a chemisorbed species whose binding energy is relatively low because of the high energetic cost of its deformation. This species will also be a good candidate for being an intermediate product in the further oxidation of methanol on Cu surfaces.

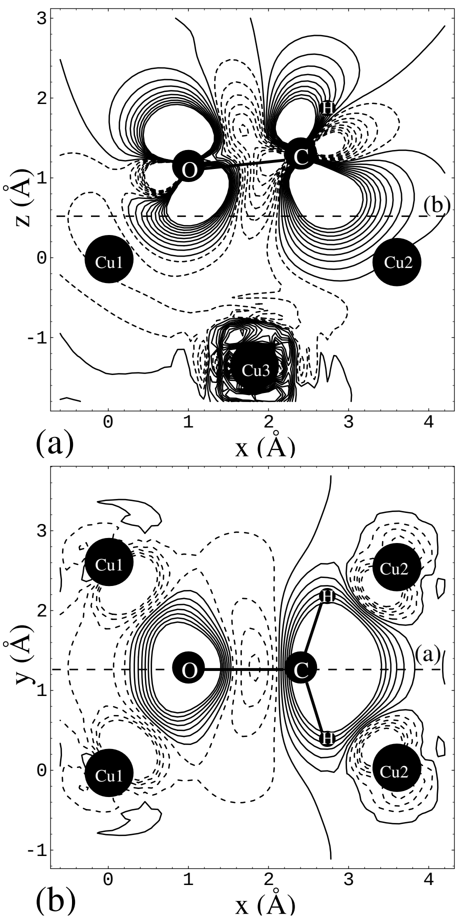

FIG. 4: Charge density difference plots of the chemisorbed formaldehyde on Cu(110). a) side view b) top view. The location of the corresponding two-dimensional cuts is shown by the dashed lines. The positions of the atoms are included in order to illustrate the geometry of the chemisorbed formaldehyde. Note that in a) the atoms denoted with Cu1 and Cu2 and the hydrogen atoms and in b) none of the shown atoms is located within the planes of the charge density difference plots.

B. Methanol partial oxidation on clean Cu(100) and Cu(110)

We have used the climbing image nudged elastic band (NEB) method [42–45] in order to determine the minimum energy pathways of the partial oxidation on clean Cu(100) and Cu(110). In the NEB scheme, the initial and final states of a reaction have to be specified. Experimentally it is well-established that the methanol oxidation on Cu is initiated by the O-H bond scission of methanol. Therefore we have assumed the following reaction path,

$$\mathrm{CH_3OH}^{(g)} \longrightarrow \mathrm{CH_3O}^{(a)} + \mathrm{H}^{(a)} \longrightarrow \mathrm{CH_2O}^{(g)} + 2\mathrm{H}^{(a)} \ . \tag{3}$$

The hydrogen atoms are supposed to remain on the surface.

The calculated reaction paths on Cu(100) and Cu(110) are illustrated in Fig. 5. The dissociation of methanol is hindered by a barrier of about 0.3 eV on Cu(100) and of about 0.7 eV on Cu(110). Interestingly, methanol is more strongly bound to Cu(110) than to Cu(100), but still the barrier for the methanol decomposition is much larger on Cu(110). This indicates the strong structure sensitivity of the reaction intermediates and transition states on Cu. We note that the hydrogen atoms interact repulsively with adsorbed methoxy and formaldehyde within a (2×2) unit cell. For the energies of the intermediate states shown in Fig. 5, we have therefore assumed that the coadsorbates are in fact separated from each other so that there is no interaction. Thus the energy difference between reactant and product states is given by

$$\Delta E = E_{\mathrm{product+H}} - E_{\mathrm{reactant}}, \tag{4}$$

where $E_{\mathrm{product+H}}$ is the sum of the adsorption energies of the isolated atomic hydrogen and the isolated product molecule.

At the transition state for the O-H bond scission on Cu(100), the methanol molecule is located at the bridge site. After dehydrogenation, methoxy moves to the energetically favorable four-fold hollow position. If we keep the molecule fixed to the four-fold hollow site, then the barrier for dehydrogenation increases from 0.34 eV to 0.88 eV. This demonstrates that it is in fact important to relax all relevant molecular degrees of freedom in the search for the minimum energy barriers.

The barrier heights of the second oxidation step are 1.38 eV on Cu(100) and 1.44 eV on Cu(110) according to the NEB calculations. This compares well with the corresponding barrier height of 1.42 eV on Cu(111) calculated previously [37]. We note that DFT cluster calculations for Cu(111) had predicted a barrier height of 1.80 eV on Cu(111) [35]. These results demonstrate that the C-H bond breaking of methanol is hindered by much larger barriers than the O-H bond breaking on Cu substrates. This is different from Pt(111) where the C-H and O-H bond scission have comparable barrier heights [58].

Details of the reaction path of the hydrogen abstraction from methoxy on Cu(110) are shown in Fig. 6. At the barrier position, the CO bond length is already strongly reduced to the value for adsorbed formaldehyde. Furthermore, the C-H bond is elongated to 2.28 Å which is considerably larger than the corresponding value of 1.64 Å on Cu(111) [37]. This indicates that at the calculated transition state configuration formaldehyde and hydrogen are already well-seperated, but that there is still a remaining electrostatic repulsive interaction which contributes to the high dissociation barrier. One can also put it differently for the reverse process, the recombination of hydrogen and formaldehyde: once the repulsive electrostatic interaction has been overcome, the recombination of formaldehyde and hydrogen on Cu(110) occurs with a large energy gain.

According to the calculated reaction barriers, adsorbed methoxy should rather associatively desorb as methanol

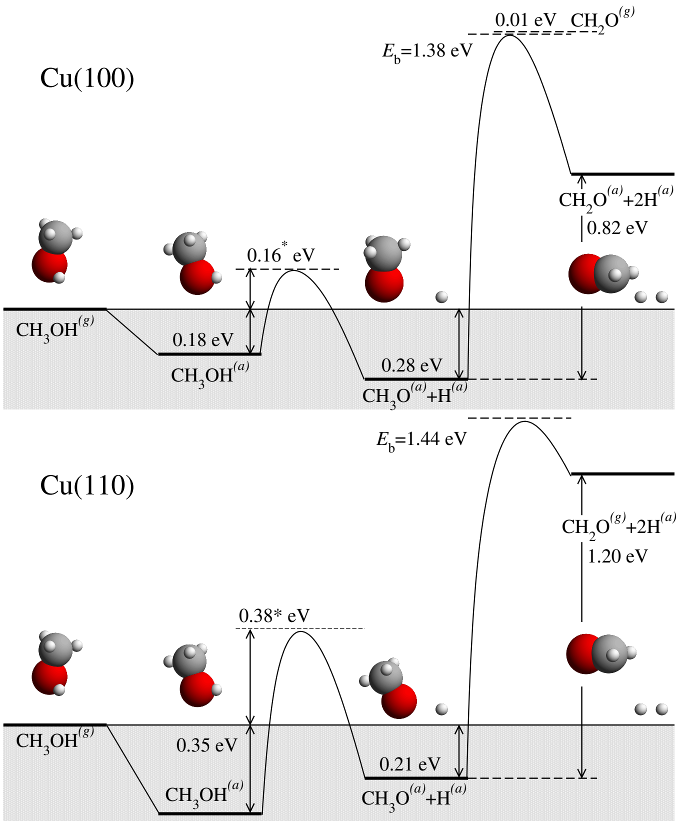

FIG. 5: Reaction pathway of methanol decomposition on clean Cu(100) and Cu(110). Whereas the the O-H bond scission is hindered only by a small activation barrier, the C-H bond scission is strongly activated.

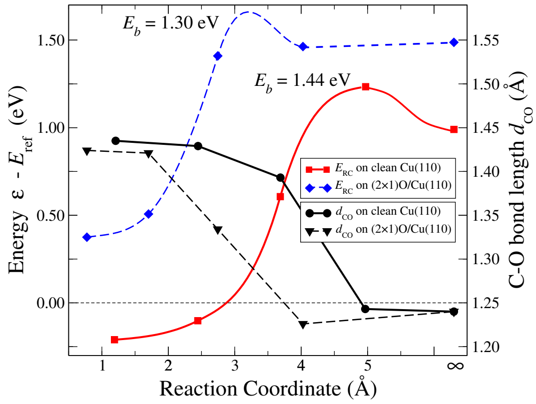

FIG. 6: Reaction barrier of the second step in the oxidation of methanol, the decomposition of methoxy into formaldehyde and hydrogen, on clean and (2×1) oxygen-covered Cu(110).

than dissociate to formaldehyde. This is in fact observed in experiments using isotope exchange [19], but only under a high concentration of hydrogen atoms on the surface. This high concentration is necessary in order to overcome the repulsion between the adsorbed hydrogen atoms and methoxy. The recombination of hydrogen and methoxy also competes with the associative desorption of H_2 [19], which have comparable desorption barriers on Cu [59, 60]. If not a sufficient amount of hydrogen is available on the surface, then formaldehyde is formed in spite of the much higher barrier [19].

However, all the calculated barrier heights for the C-H bond scission are still significantly larger than the experimentally derived results of 0.92 eV for Cu(110) [23] and 1.06 eV for oxygen Cu(111) [47]. It should be noted that these experiments have been performed on oxygen predosed surfaces which might have influenced the barrier heights. As we will show in the next section, we find a minor influence of adsorbed oxygen on the hydrogen abstraction barrier from methoxy. We note that the barrier heights determined with the NEB method did not include any relaxations of the substrate. Our calculations show that the lowering or the total energy induced by the adsorbates on Cu(110) are 70 meV for methoxy and 100 meV for chemisorbed formaldehyde. Hence we estimate that the influence of the surface relaxations on the barrier heights is below 100 meV.

Thus there is still a remaining discrepancy between theory and experiment, as far as the barrier for C-H bond scission is concerned. It is a well-known fact that DFT calculations using the GGA for the exchange-correlation effects overestimate the barrier for C-H bond scission in many systems. For example, the barrier for the C-H bond breaking of ethylene (C_2H_4) to vinyl (C_2H_3) on Pd(111) was calculated to be 1.5 eV by DFT-GGA(PW91) calculations [61] while experimental values are 0.65-0.75 eV on Pd(100) [62]. For the methane (CH_4) decomposition on Ni(111), the DFT-GGA dissociation barrier is about 1.0 eV [63], whereas in molecular beam experiments activation energies of 0.65 eV on Ni(100) and 0.75 eV on Ni(111) were found (see [64] and references therein). For the CH_4/Ni system, *ab initio* quantum chemistry results for the dissociation barrier are much closer to experiment, namely 0.67 eV for Ni(100) [65] and 0.7 eV for Ni(111) [66]. We conclude that while the exact barrier height for the C-H bond scission of methoxy on Cu might be overestimated by our DFT calculations, nevertheless the qualitative trends are in good agreement with the experiment.

C. Methanol partial oxidation on oxygen covered copper surfaces

Experimentally it is well-established that oxygen on copper acts as a promoter for the oxidation of methanol. The conversion of methanol to formaldehyde is maximal on various Cu surfaces for an oxygen coverage of $\theta_O \cong 1/4$ [19, 47, 67]. For lower coverages, methoxy formation and water desorption are dominant whereas higher oxygen coverages lead to relatively inert surfaces.

As far as the influence of oxygen on the methanol dehydrogenation is concerned, we have mainly focused on the Cu(110) surface. The methanol adsorption on

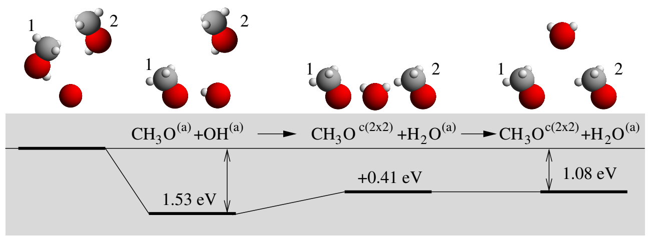

FIG. 7: Initial steps of the methanol dehydrogenation on oxygen-covered Cu(110). Sequentially approaching methanol molecules are dehydrogenated and the hydrogen is removed via water desorption.

oxygen-covered Cu(100) will be addressed in the next section. The oxygen-covered Cu(110) surface exhibits a (2×1) "added row" reconstruction consisting of Cu-O-Cu chains [68, 69]. Still we first considered "isolated" oxygen adatoms in a $p(2\times2)$ structure on the open Cu(110) surface. Thus the results might also be relevant for the understanding of the proposed suboxide species on Cu/ZnO catalysts [8].

The initial steps of the methanol adsorption are depicted in Fig. 7. The oxygen atoms are located in the pseudo three-fold hollow sites on Cu(110). As we showed above, methoxy forms a stable $c(2\times2)$ structure on Cu(110), in agreement with STM studies [22, 28, 29]. Therefore we have considered the sequential adsorption of two methanol molecules per $p(2\times2)$O/Cu(110) surface unit cell. As Fig. 7 shows, the presence of the oxygen adatom leads to the spontaneous breaking of the methanol O-H bond,

$$\mathrm{CH_3OH}^{(g)} + \mathrm{O}^{(a)} \longrightarrow \mathrm{CH_3O}^{(a)} + \mathrm{OH}^{(a)} \qquad (5)$$

In other words, the oxygen adatom acts as a strong Brønsted base that abstracts the hydroxyl hydrogen of methanol [70]. This results in a large energy gain of 1.53 eV upon the dissociative adsorption of methanol. According to our calculations there is still an attractive interaction between methoxy and OH per $p(2\times2)$ unit cell of 0.31 eV compared to the isolated adsorbates. The second dissociative adsorption of a methanol molecule in the (2×2) unit cell forming a $c(2\times2)$ methoxy structure plus one adsorbed water molecule is endothermic by 0.41 eV. However, this structure is energetically almost degenerate with the $c(2\times2)\mathrm{CH_3O}$/Cu(110) structure on Cu(110) and the water molecule desorbed into the gas phase. This means that the overall reaction

$$2\mathrm{CH_3OH}^{(g)} + \mathrm{O}^{(a)} \longrightarrow 2\mathrm{CH_3O}^{c(2\times2)} + \mathrm{H_2O}^{(g)}. \qquad (6)$$

is exothermic by 1.08 eV.

We note that we also investigated an alternative pathway for the reaction (6) which might be relevant for smaller methanol exposures. The methanol adsorption energies increases to 0.83 eV on a $p(2\times2)$OH/Cu(110) surface, i.e. after methoxy and OH have been separated after the first reaction step (5). This means that OH attracts methanol, without, however, inducing a spontaneous methanol decomposition. Furthermore, methanol decomposition and subsequent water desorption from this structure requires a desorption energy of 1.06 eV, i.e. methanol desorption is energetically more favorable than the methanol decomposition and water desorption.

Hence the scenario described in Fig. 7 seems to be the more realistic one. The water desorption leads to the removal of both surface hydrogen and surface oxygen. In fact, this scenario agrees well with experimental observations that water desorbs at lower temperatures than those at which the methoxy-hydrogen recombination occurs [19]. It also gives a rationalization for the STM experiments which find well-segregated methoxy and surface oxygen islands [22, 28, 29] with the development of the ordered methoxy structures accompanied by the removal of oxygen [29].

As far as the further decomposition of methoxy on Cu(110) is concerned, we find that in the (2×2) structure the adsorbed oxygen does not lower the barrier for the C-H bond scission to hydrogen and formaldehyde. Hence the reaction barrier for the methoxy decomposition on clean Cu(110) of 1.44 eV shown in Fig. 5 is also relevant for the oxygen-covered surface. Still, the reverse route of direct associative methanol desorption is no longer available since the surface hydrogen has been removed together with the oxygen via water desorption. In that sense the oxygen dosage effectively leads to the formaldehyde formation.

The TPD experiments [19] show that both methanol and formaldehyde are produced simultaneously according to the reaction scheme

$$2\mathrm{CH_3O}^{c(2\times2)} \longrightarrow \mathrm{CH_3OH}^{(g)} + \mathrm{CH_2O}^{(g)}\ . \qquad (7)$$

In addition, also H_2 is formed. All products desorb between 350 K and 375 K. According to our DFT results, the total reaction (7) requires an energy $\Delta E = 1.9$ eV. On the other hand, STM experiments have found that prolonged exposure of oxygen leads to the displacement of methoxy adsorbates from the surface by oxygen [29]. We have tried to model this by determining the reaction barrier for methoxy decomposition on the (2×1) oxygen-covered Cu(110) surface. The methoxy coverage was selected to be $\theta = 0.25$ to reflect the findings of the STM experiments that the methoxy molecules are replaced along the $\langle 001\rangle$ direction by oxygen exposure.

The energetics along the methoxy decomposition pathway are also included in Fig. 6. The whole energy curve is shifted up with respect to the clean surface results which reflects the repulsive interaction of reactants and products with the adsorbed oxygen at this high coverage. The energy difference ΔE between product and reactant states is reduced from 1.20 eV on the clean surface to 1.13 eV on the oxygen-covered surface. Furthermore, also the reaction barrier is lowered from 1.44 eV to 1.30 eV. Figure 6 demonstrates that at the oxygen-covered Cu(110) surface the CO bond length decreases much more rapidly than on clean Cu(110). This is an indication of the reduced methoxy-surface interaction [71] caused by the presence of oxygen on the surface. The lowering of the methoxy decomposition barrier on the oxygen-covered surface can qualitatively explain the replacement of adsorbed methoxy by continuing oxygen supply found in STM experiments [29].

D. Substrate strain effects on the methanol oxidation

Using a X-ray diffraction line profile analysis, Günter *et al.* demonstrated that the microstrain and the lattice spacing of the Cu particles of a Cu/ZnO catalyst rises with increasing Zn concentration [7]. For a Zn concentration of 80 mol-% the lattice expansion was 0.35 %. This lattice expansion was shown to correlate with the methanol synthesis activity of the catalyst. Previous experiments [9, 10, 16] and DFT calculations [11–15] have confirmed the influence of substrate strain on the adsorption of atoms and molecules. A lattice expansion of d-band metal leads to an upshift of the center of the d-band [11] which results in a higher reactivity of the surface according to the d-band model [18]. For expanded Cu surfaces, DFT calculations have indeed found higher binding energies in high-coordinated adsorption sites and lower dissociation barriers for oxygen [12] and hydrogen [13].

For Cu(110), we have determined the adsorption energies for the reaction intermediates of the partial oxidation for a Cu lattice expanded by 4%. The results are compared with the corresponding values on Cu(110) at its calculated equilibrium spacing of 3.64 Å in Table II. It is obvious that the adsorption energies of methanol, methoxy and formaldehyde are hardly influenced by the lattice strain. Their binding energies increase only by 20-30 meV for such a significant lattice expansion of 4 %. The OH adsorption energy and in particular the oxygen adsorption energies, however, are considerably modified. Oxygen atoms are more strongly bound on expanded Cu(110) by almost 0.2 eV which compares well for the corresponding results on expanded Cu(111) [12].

The enhanced binding energy of atomic oxygen has interesting consequences for the energy gain in the dissociative adsorption of methanol on the expanded

a(Å)		$\frac{1}{2}O_2$	CH_3OH	CH_3O	CH_2O	OH
	E_{ads}(eV)	−2.46	−0.35	−2.98	−0.22	−3.49
3.64	h_{Cu-O}(Å)	0.63	1.84	1.44	1.71	1.43
	d_{Cu-O}(Å)	1.89	2.34	1.95	2.16	1.95
	E_{ads}(eV)	−2.64	−0.37	−3.01	−0.25	−3.56
3.80	h_{Cu-O}(Å)	0.59	1.84	1.31	1.66	1.35
	d_{Cu-O}(Å)	1.88	2.36	1.94	2.15	1.95

TABLE II: Adsorption energies E_{ads}, adsorption height h_{Cu-O} and distance to the nearest Cu atom d_{Cu-O} of various surface adsorbates on Cu(110) as a function of the lateral lattice constant a.

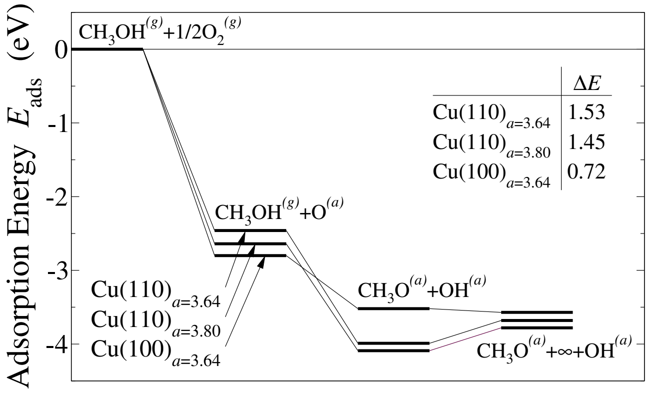

FIG. 8: Energetics of the oxygen adsorption and the dissociative adsorption of methanol on Cu(110) as a function of the lattice constant a. In addition, the corresponding energies for Cu(100) with its equilibrium lattice constants are included. The last state corresponds to the independent adsorption of methoxy and hydroxyl, i.e. for infinite separation of both species on the surface. The inset lists the energy gain ΔE in eV upon the dissociative adsorption of methanol on the oxygen-covered Cu surfaces.

(2×2)O/Cu(110) surfaces which are illustrated in Fig. 8. The binding energies of methoxy and hydroxyl are increased by 0.1 eV for the adsorbates both within a (2×2) unit cell as well as for infinite separation, in agreement with the predictions of the d-band model. However, since the increase in the adsorption energy of oxygen alone is even larger, the energy gain ΔE upon the dissociative adsorption of methanol is reduced from 1.53 eV to 1.45 eV on the expanded oxygen covered surface. This implies that the reactivity of the oxygen-covered Cu surface towards the methanol O-H bond breaking is governed by the bonding strength of the adsorbed atomic oxygen. Less tightly bound oxygen is more active for methanol decomposition.

This also partially explains the much lower reactivity of the oxygen-covered Cu(100) surface compared to Cu(110) for the methanol decomposition. On Cu(100), oxygen atoms are stronger bound by about 0.3 eV than on Cu(110) (see Fig. 8). Consequently, there is a much smaller energy gain upon the dissociative adsorption of methanol of only 0.72 eV which is, however, also due to the geometry of the Cu(100) surface which is unfavorable for the combined adsorption of methoxy and hydroxyl within a (2×2) unit cell.

The reduced binding energy of the methoxy-hydroxyl complex on the expanded oxygen-covered Cu surface would in fact enhance the rate of methanol synthesis, in agreement with the experiment [7], once methoxy and OH have approached each other on the substrate. However, it should be noted that the Cu lattice expansion found in the Cu/ZnO catalysts is much smaller than the one that we assumed for our calculations. Still the qualitative conclusions should be valid in general: on an expanded substrate, the *total* binding energies of *all* involved atoms and molecules is enhanced, but the increase depends on the specific reaction intermediates. Hence there is no clear trend for a particular reaction barrier or energy difference as a function of lattice strain.

IV. CONCLUSIONS

Methanol decomposition pathways overs various Cu surfaces have been addressed by DFT calculations. The rate-limiting step in the partial oxidation of methanol is the decomposition of methoxy into formaldehyde and hydrogen. While this barrier is not reduced by the presence of oxygen on the surface, oxygen still enhances the formaldehyde formation by stabilizing the methoxy intermediate and removing the hydrogen via water desorption. Tensile strain leads to enhanced binding energies of the reaction intermediates, however, the stronger bound oxygen atoms on the expanded surface are less active with respect to the methanol O-H bond scission.

The information about the calculated reaction intermediates and the transition barriers of the partial oxidation of methanol on Cu are now detailed enough for a kinetic modeling. Such a study is under way at the moment.

Acknowledgments

This work has been supported by the German Academic Exchange Service (DAAD) and the German Science Foundation (DFG, GR1503/12-1).

---

[1] Peppley, B.; Amphlett, J.; Kearns, L.; Mann, R. *Appl. Catal. A* **1999**, *179*, 21.
[2] Peppley, B.; Amphlett, J.; Kearns, L.; Mann, R. *Appl. Catal. A* **1999**, *179*, 31.
[3] Vanden Bussche, K. M.; Froment, G. G. *J. Catal.* **1996**, *161*, 1.
[4] Klier, K. *Adv. Catal.* **1982**, *31*, 243.
[5] Chinchen, G. C.; Waugh, K. C.; Whan, D. A. *Appl. Catal.* **1986**, *25*, 101.
[6] Chinchen, G. C.; Hay, C. M.; Vandervell, H. D.; Waugh, K. C. *J. Catal.* **1987**, *103*, 79.
[7] Günter, M.; Ressler, T.; Bems, B.; Büscher, C.; Genger, T.; Hinrichsen, O.; Muhler, M.; Schlögl, R. *Catal. Lett.* **2001**, *71*, 37.
[8] Knop-Gericke, A.; Hävecker, M.; Schedel-Niedrig, T.; Schlögl, R. *Top. in Catal.* **2001**, *15*, 27.
[9] Gsell, M.; Jakob, P.; Menzel, D. *Science* **1998**, *280*, 717.
[10] Jakob, P.; Gsell, M.; Menzel, D. *J. Chem. Phys.* **2001**, *114*, 10075.
[11] Mavrikakis, M.; Hammer, B.; Nørskov, J. K. *Phys. Rev. Lett.* **1998**, *81*, 2819.
[12] Xu, Y.; Mavrikakis, M. *Surf. Sci.* **2001**, *494*, 131.
[13] Sakong, S.; Groß, A. *Surf. Sci.* **2003**, *525*, 107.
[14] Roudgar, A.; Groß, A. *Phys. Rev. B* **2003**, *67*, 033409.
[15] Roudgar, A.; Groß, A. *J. Electronal. Chem.* **2003**, *548*, 121.
[16] Schlapka, A.; Lischka, M.; Groß, A.; Käsberger, U.; Jakob, P. *Phys. Rev. Lett.* **2003**, *91*, 016101.
[17] Ohno, S. Y.; Yagyuu, K.; Nakatsuji, K.; Komori, F. *Surf. Sci.* **2004**, *554*, 183.
[18] Hammer, B.; Nielsen, O.; Nørskov, J. *Surf. Sci.* **1995**, *343*, 211.
[19] Wachs, I. E.; Madix, R. J. *J. Catal.* **1978**, *53*, 208.
[20] Bowker, M.; Madix, R. J. *Surf. Sci.* **1980**, *95*, 190.
[21] Sexton, B. A.; Hughes, A. E.; Avery, N. R. *Surf. Sci.* **1985**, *155*, 366.
[22] Leibsle, F. M.; Francis, S. M.; Davis, R.; Xiang, N.; Haq, S.; Bowker, M. *Phys. Rev. Lett.* **1994**, *72*, 2569.
[23] Madix, R. J.; Telford, S. G. *Surf. Sci.* **1995**, *328*, L576.
[24] Carley, A. F.; Davies, P. R.; Mariotti, G. G.; Read, S. *Surf. Sci.* **1996**, *364*, L525–L529.
[25] Poulston, S.; Jones, A. H.; Bennett, R. A.; Bowker, M. *J. Phys.: Condens. Matter* **1996**, *8*, L765–L771.
[26] Davies, P. R.; Mariotti, G. G. *Catal. Lett.* **1997**, *43*, 261.
[27] Bowker, M.; Poulston, S.; Bennett, R. A.; Jones, A. H. *Catal. Lett.* **1997**, *43*, 267.
[28] Silva, S. L.; Lemor, R. M.; Leibsle, F. M. *Surf. Sci.* **1999**, *421*, 135.
[29] Silva, S. L.; Lemor, R. M.; Leibsle, F. M. *Surf. Sci.* **1999**, *421*, 146.
[30] Karolewski, M. A.; Cavell, R. G. *Appl. Surf. Sci.* **2001**, *173*, 151.
[31] Ammon, C.; Bayer, A.; Held, G.; Richer, B.; Schmidt, T.; Steinrück, H. P. *Surf. Sci.* **2002**, *507*, 845.
[32] Wachs, I. E.; Madix, R. J. *Surf. Sci.* **1979**, *84*, 375.
[33] Witko, M.; Hermann, K. *J. Chem. Phys.* **1994**, *101*, 10173.
[34] Nakatsuji, K.; Hu, Z.-M. *Int. J. Quantum. Chem.* **2000**, *77*, 341.
[35] Gomes, J. R. B.; Gomes, J. A. N. F.; Illas, F. *Surf. Sci.* **1999**, *443*, 165.
[36] Gomes, J. R. B.; Gomes, J. A. N. F. *Surf. Sci.* **2001**, *471*, 59.
[37] Greeley, J.; Mavrikakis, M. *J. Catal.* **2002**, *208*, 291.
[38] Perdew, J. P.; Chevary, J. A.; Vosko, S. H.; Jackson, K. A.; Pederson, M. R.; Singh, D. J.; Fiolhais, C. *Phys. Rev. B* **1992**, *46*, 6671.
[39] Kresse, G.; Furthmüller, J. *Phys. Rev. B* **1996**, *54*, 11169.
[40] Vanderbilt, D. *Phys. Rev. B* **1990**, *41*, 7892.
[41] Kresse, G.; Hafner, J. *J. Phys.: Condens. Matter* **1994**, *6*, 8245.
[42] Schenter, G.; Mills, G.; Jónsson, H. *J. Chem. Phys.* **1994**, *101*, 8964.
[43] Mills, G.; Jónsson, H.; Schenter, G. *Surf. Sci.* **1995**, *324*, 305.
[44] Henkelman, G.; Jónsson, H. *J. Chem. Phys.* **2000**, *113*, 9978.
[45] Henkelman, G.; Uberuaga, B. P.; Jónsson, H. *J. Chem. Phys.* **2000**, *113*, 9901.
[46] Henkelman, G.; Jónsson, H. *J. Chem. Phys.* **1999**, *111*, 7010.
[47] Russell Jr., J. N.; Gates, S. M.; Yates Jr., J. T. *Surf. Sci.* **1985**, *163*, 516.

[48] Sexton, B. A.; Hughes, A. E. *Surf. Sci.* **1984**, *140*, 227.
[49] Clarke, D. B.; Lee, D.; Sandoval, M. J.; Bell, A. T. *J. Catal.* **1994**, *150*, 81.
[50] Ryberg, R. *Phys. Rev. Lett.* **1982**, *49*, 1579.
[51] Jackels, C. F. *J. Chem. Phys.* **1985**, *82*, 311.
[52] Ricken, D. E.; Somers, J. Robinson, A. W.; Bradshaw, A. M. *Faraday Disc. Chem. Soc.* **1990**, *89*, 291.
[53] Rodriguez, J. A. *Surf. Sci.* **1992**, *273*, 385.
[54] Bader, M.; Puschmann, A.; Hasse, J. *Phys. Rev. B* **1986**, *33*, 7336.
[55] Holub-Krappe, E.; Prince, K. C.; Horn, K.; Woodruff, D. P. *Surf. Sci.* **1986**, *173*, 176.
[56] Dastoor, H. E.; Gardner, P.; King, D. A. *Chem. Phys. Lett.* **1993**, *209*, 493.
[57] Singh, J.; Walter, W. K.; Atrei, A.; King, D. A. *Chem. Phys. Lett.* **1991**, *185*, 426.
[58] Greeley, J.; Mavrikakis, M. *J. Am. Chem. Soc.* **2004**, *126*, 3910–3919.
[59] Hammer, B.; Scheffler, M.; Jacobsen, K.; Nørskov, J. *Phys. Rev. Lett.* **1994**, *73*, 1400.
[60] Groß, A.; Hammer, B.; Scheffler, M.; Brenig, W. *Phys. Rev. Lett.* **1994**, *73*, 3121.
[61] Pallassana, V.; Neurock, M.; Lusvardi, V. S.; Lerour, J. J.; Kragten, D. D.; van Santen, R. A. *J. Phys. Chem. B* **2002**, *106*, 1656.
[62] Stuve, E. M.; Madix, R. J. *J. Phys. Chem.* **1985**, *89*, 105.
[63] Kratzer, P.; Hammer, B.; Nørskov, J. K. *J. Chem. Phys.* **1996**, *105*, 5595.
[64] Abbott, H. L.; Bukoski, A.; Kavulak, D. F. Harrison, I. *J. Chem. Phys.* **2003**, *119*, 6407.
[65] Swang, O.; Faegri, K.; Gropen, O.; Wahlgren, U.; Siegbahn, P. *Chem. Phys.* **1991**, *156*, 379.
[66] Yang, H.; Whitten, J. L. *J. Chem. Phys.* **1992**, *96*, 5529.
[67] Sexton, B. A. *Surf. Sci.* **1979**, *88*, 299.
[68] Coulman, D. J.; Wintterlin, J.; Behm, R. J.; Ertl, G. *Phys. Rev. Lett.* **1990**, *64*, 1761.
[69] Jensen, F.; Besenbacher, F.; Laegsgaard, E.; Stensgaard, I. *Phys. Rev. B* **1990**, *41*, 10233.
[70] Outka, D. A.; Madix, R. J. *J. Am. Chem. Soc.* **1987**, *109*, 1708.
[71] Amemiya, K.; Kitajima, Y. *Phys. Rev. B* **1999**, *59*, 2307.